Journal of Applied Polymer Science

Synergistic effect of silica nanoparticles in the matrix of a poly(ethylene glycol) diacrylate coating layer for the surface modification of polyamide nanofiltration membranes

Vahid Vatanpour, Mostafa Kavian
Faculty of Chemistry, Kharazmi University, 15719-14911 Tehran, Iran
Correspondence to: V. Vatanpour (E-mail: vahidvatanpour@khu.ac.ir or vahidvatanpoor@yahoo.com)

ABSTRACT: In this study, a commercial polyamide nanofiltration membrane was modified by a combination of poly(ethylene glycol) diacrylate (PEGDA) *in situ* polymerization and silica (SiO_2) nanoparticles. The PEGDA layer was polymerized on the surface of the membranes alone or mixed with SiO_2 nanoparticle. The surface modification influence on the water flux, salt rejection, and antifouling behavior was investigated. The effects of the nanoparticles and PEGDAylation on the membrane properties were characterized by Fourier transform infrared spectroscopy, contact angle measurement, and scanning electron microscopy analyses. The membranes that were in contact with 30 wt % PEGDA and then treated with ultraviolet light for 5 min had a better water flux than the unmodified membrane. The fouling resistance of the membranes to a foulant solution containing bovine serum albumin, humic acid, and sodium sulfate were studied, and the results show that the membrane with 30 wt % PEGDA had better antifouling properties. After the weight percentage of PEGDA for the prepolymerization solution was optimized (30 wt % was the best), the SiO_2 nanoparticle concentration in the prepolymerization matrix was optimized. The presence of SiO_2 nanoparticles in the PEGDA layer increased the membrane flux. The maximum water flux and good antifouling properties were obtained for 0.5 wt % SiO_2 nanoparticles in a 30 wt % PEGDA layer. © 2016 Wiley Periodicals, Inc. J. Appl. Polym. Sci. **2016**, *133*, 43793.

KEYWORDS: coatings; membranes; nanoparticles; nanowires and nanocrystals

Received 23 February 2016; accepted 17 April 2016
DOI: 10.1002/app.43793

INTRODUCTION

Nanofiltration (NF) is a membrane filtration process that is mostly used for the separation of multivalent salts from univalent salts. It is a membrane separation process that is widely used in the treatment of water and wastewater, especially for water-softening applications.[1] In the drinking water industry, NF has been generally applied to the removal of hardness, natural organic material, and micropollutants.[2]

NF membranes have features between reverse osmosis (RO) and ultrafiltration. They have a partly high flux and low pressure with a size cutoff on the molecular scale between 0.5 to 2 nm.[3] NF membranes are commonly thin-film composite (TFC) membranes manufactured from a negatively charged aromatic polyamide (PA) interfacially polymerized onto a porous support.

Membrane fouling is a major barrier to the efficient operation of NF membranes in industry.[4] The charged nature of the PA interfacial layer causes NF membranes to be susceptible to fouling by suspended or solvated charged foulants.[5] The fouling of NF membrane leads to a lot of deleterious influences, including a reduction in water production that is due to a gradual decrease in flux, an increase in the applied pressure needed for a constant amount of water production, a decline in the permeate quality, and a gradual membrane degradation that leads to to a shorter membrane life[4] and causes a considerable loss in the productivity and additional operational expenses.[6] Membrane fouling can reduce the permeate flux and decrease the selectivity of the membranes.[7] The properties of fouled membranes can be recovered relatively well by cleaning; however, this method increases the operation costs and decreases the membrane lifetime. An effective way to relieve these problems and promote the application of the membranes is to enhance their antifouling characteristics.[8–16] So far, a lot of methods have been examined; these include surface modification with coating,[8,9] grafting[10–12] or chemical treatment,[13] the incorporation of organic additives[14] or nanoparticles[15] to the PA layer, and the fabrication of membranes with antifouling materials.[16] The majority of these methods result in the development of the membrane surface properties with hydrophilic modifiers.

Among different hydrophilic modifiers, poly(ethylene glycol) (PEG) or poly(ethylene oxide) (PEO) and their derivatives have

been examined extensively.[9–12] PEG is an uncharged polymer with the chemical formula HO—(CH_2CH_2O)n—H. Its remarkable antifouling ability has been proven to be due to the hydrophilicity and flexible long chains in aqueous medium.[17] Many studies have been conducted on the application of these types of polymers for the modification of the membranes in different procedures, including the grafting, incorporation, or coating of PEG chains on the membrane surfaces, and these studies have had encouraging results.[18–21]

Poly(ethylene glycol) diacrylate (PEGDA), whose structure is shown in Figure 1, is a derivative of PEG with repeated ethylene oxide units and active end groups. Irradiation from an ultraviolet (UV) lamp in the presence of a photoinitiator could polymerize PEGDA. There are some reports on a number of crosslinked PEO rubbers with PEGDA as a major material for gas separation.[22–25] Nevertheless, the characteristics of crosslinked PEGDA membranes for water treatment have scarcely been presented. However, an investigation of a crosslinked PEO fouling-resistant coating materials for oil/water separation was presented.[26] The crosslinked PEGDA showed a high water permeability and good fouling resistance to oil/water mixtures.

Kang *et al.*[27] prepared crosslinked PEGDA (molecular weight = 302 g/mol) membranes by means of UV-induced polymerization with the addition of variety of ethanol in a prepolymerization solution without support for ultrafiltration application. Bovine serum albumin (BSA) fouling and a preliminary solvent soaking test showed that the fabricated membranes presented good solvent-resistant and antifouling properties. Sagle *et al.*[9] synthesized a series of crosslinked PEG-based hydrogels with PEGDA as a crosslinker and acrylic acid, 2-hydroxyethyl acrylate, or PEG acrylate as comonomers for the preparation of surface-coated RO membranes to mitigate membrane fouling. The coated membranes exhibited low fouling in oil/water emulsion filtration.

However, coating, *in situ* polymerization, or grafting of a polymer layer on a membrane surface can cause a reduction in the membrane permeability[9,18]; this is due to an increase in the membrane thickness and the blocking of some pores. To overcome this problem, the application of some nanoparticles can improve the hydrophilicity, porosity, and permeability of the coated layer.[28,29] The synergistic effect of a hydrophilic polymer coating and nanoparticles can improve the antifouling properties of the membranes. For example, Ag nanoparticles were used in the matrix of PEGylated dendrimer nanocomposite coatings to prepare TFC membranes to decrease both protein and bacteria fouling.[30]

In this study, a commercial PA NF membrane was modified by PEGDA *in situ* polymerization with or without silica (SiO_2) nanoparticles. With the *in situ* polymerization method, first, the monomers were diffused among the supporting polymer chains, and next, when they were polymerized, the prepared new polymer was trapped among the support polymer chains and attached to the support surface. First, the PEGDA polymerization conditions were optimized, and next, different concentrations of SiO_2 nanoparticles were added to the prepolymerization solution. The effects of this layer on the membrane hydrophilicity, surface morphology, rejection, flux, and antifouling properties were examined.

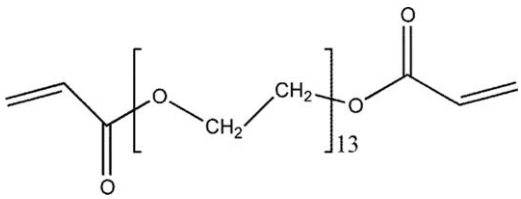

Figure 1. Chemical structures of PEGDA.

EXPERIMENTAL

Materials

PEGDA, with a molecular weight of 708 g/mol, was provided by Shin-Nakamura Chemical Co., Ltd. BSA and sodium sulfate (Na_2SO_4) were purchased from Merck, and humic acid was prepared from Sigma-Aldrich. 1-Hydroxycyclohexyl phenyl ketone as a photoinitiator was obtained from Aldrich. All other chemicals were analytically pure grade. RO water (1 μS/cm) was used as a solvent of PEGDA and for other uses.

The flat-sheet commercial PA NF membrane was cut from a CSM NE4040 module manufactured in South Korea. SiO_2 nanoparticles with particle sizes of 20–30 nm were purchased from US Nano Co.

Membrane Surface Modification

For the surface modification of the PA NF membrane, first, the PEGDA *in situ* polymerization conditions were optimized on the basis of the water flux and fouling resistance, and next, different concentrations of SiO_2 nanoparticles were added to the optimum prepolymerization solution. For the preparation of the prepolymerization solutions, at the beginning, different PEGDA monomer concentrations (10, 20, 30, 50, and 75 wt %) were weighed, and then, a 0.1 wt % initiator of 1-hydroxycyclohexyl phenyl ketone on the basis of the PEGDA amount was added. Then, the mixture was rigorously stirred for 1 h. Next, water was poured into the previous solutions until they reached a certain volume.

For the *in situ* polymerization of PEGDA on the membrane surface, the flat-sheet membranes were sandwiched between a PTFE plate and a silicon rubber O-ring with thickness of 1 cm. Then, the prepolymerization solutions were poured onto the surface of the membranes, and they were allowed to remain in contact for 10 min. After the exposure time was finished, we drained an excess of the prepolymerization solution by keeping it vertical. To initiate polymerization, membranes in the clamps were placed in a 312-nm UV-light chamber for 5 min. The obtained membranes were immersed in a large amount of water for at least 2 h and were tested next.

After the concentration of PEGDA monomer was optimized, the concentration of SiO_2 nanoparticles in PEGDA (0.1, 0.2, 0.5, 1, and 2 wt % relative to the PEGDA amount) was optimized. For this purpose, first, SiO_2 nanoparticles were dispersed in water with a bath sonicator for 30 min. Next, a 30 wt % PEGDA/photoinitiator solution was added to these suspensions.

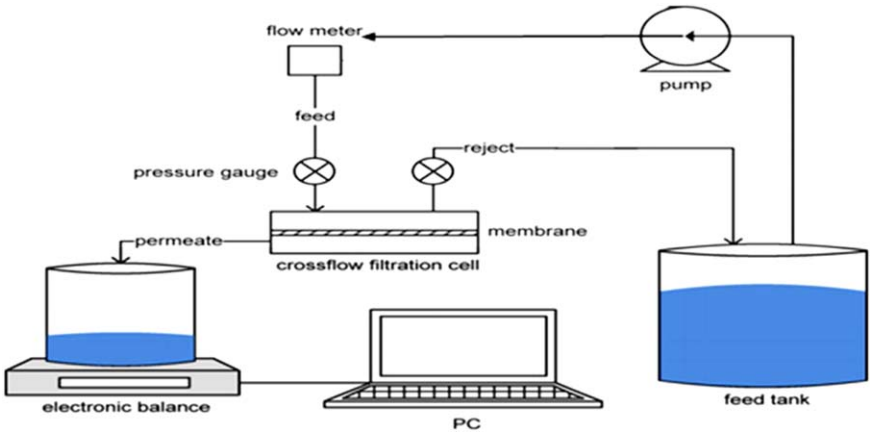

Figure 2. Crossflow filtration setup. PC = personal computer. [Color figure can be viewed in the online issue, which is available at wileyonlinelibrary.com.]

Membrane Surface Characterization

Fourier Transform Infrared (FTIR) Spectroscopy. To study the chemical composition changes and surface chemical functionality between the modified and unmodified membranes and confirm the *in situ* polymerization of PEGDA onto the NF membrane surface, ABB Bomem FTIR spectroscopy was used. The membrane samples were dried in a vacuum oven before analysis. IR spectra of the membranes were recorded in the wave-number range 400–4000 cm^{-1} at 25 °C.

Scanning Electron Microscopy (SEM). The surface and cross-sectional morphologies of the unmodified and PEGDA/SiO_2 modified membranes were examined by SEM with a Tescan Vega scanning microscope. The membrane samples for the cross-sectional SEM analysis were initially dried in air and were then frozen in liquid nitrogen for 10–15 s and fractured. After which, the sample surfaces were coated with a thin layer of gold before the images were obtained. The nonwoven polyester could not be broken in liquid nitrogen. Therefore, the membrane layer was separated from the nonwoven polyester fabric and was then broken in liquid nitrogen.

Contact Angle Measurement. The hydrophilicity of the membrane surface was determined on the basis of pure water contact angle measurement. A total of 2 μL of deionized water was dropped carefully onto the surface of the membranes with a microsyringe. The water contact angle was measured at 25 °C by the sessile drop method on a contact angle goniometer equipped with video capture (G10, Kruss, Germany). The results of at least five measurements were averaged to obtain a reliable value.

Filtration Experiments and Crossflow Filtration System

A crossflow filtration system was used to perform the tests; the results are shown in Figure 2. The NF membranes were placed in a stainless steel filtration cell, and the feed solution was passed across a 4 × 9-cm^2 membrane surface at a flow rate of 120 L/h. The pressure through the membranes was held at 10 bar. The temperature of the feed solution was kept at 25 °C with a thermostatic bath. The retentate stream was sent back to the feed source, and the permeate was gathered in a dish and placed on an electronic mass balance (AND GF-6100), which was connected to a personal computer. The difference in the mass of the permeate according to time was recorded by a computer connected to the balance that could calculate the flux.

We obtained the permeation flux (J) of each membrane sample by weighing the gained permeate during a predetermined time and calculating it by the following equation[31]:

$$J - \frac{w}{A\Delta t} \quad (1)$$

where w is the weight of the gained permeate during a predetermined NF operation time (Δt) and A is the membrane area. First, the modified membranes were compacted with RO water at 15 bar for about 30 min until the flux was stabilized. Then, the pressure was lowered to 10 bar, and we measured the flux of pure water by weighing the permeate.

Fouling Experiments

Membrane fouling tests were conducted through the crossflow setup of an aqueous foulant solution containing 500 mg/L BSA, 2000 mg/L Na_2SO_4, and 500 mg/L humic acid. The antifouling properties of the membranes were assessed by the monitoring of the permeation flux for a period time of 24 h. After the pure water filtration test was completed, the feed tank was emptied, and the foulant solution was added to it. Then, the system was turned on, the pressure was set to 10 bar, and the foulant solution flux was recorded by a computer for 24 h. The permeate

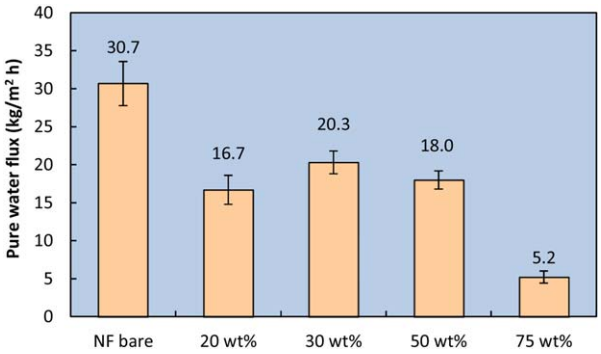

Figure 3. Effect of the PEGDA concentration on the pure water flux of the prepared membranes. [Color figure can be viewed in the online issue, which is available at wileyonlinelibrary.com.]

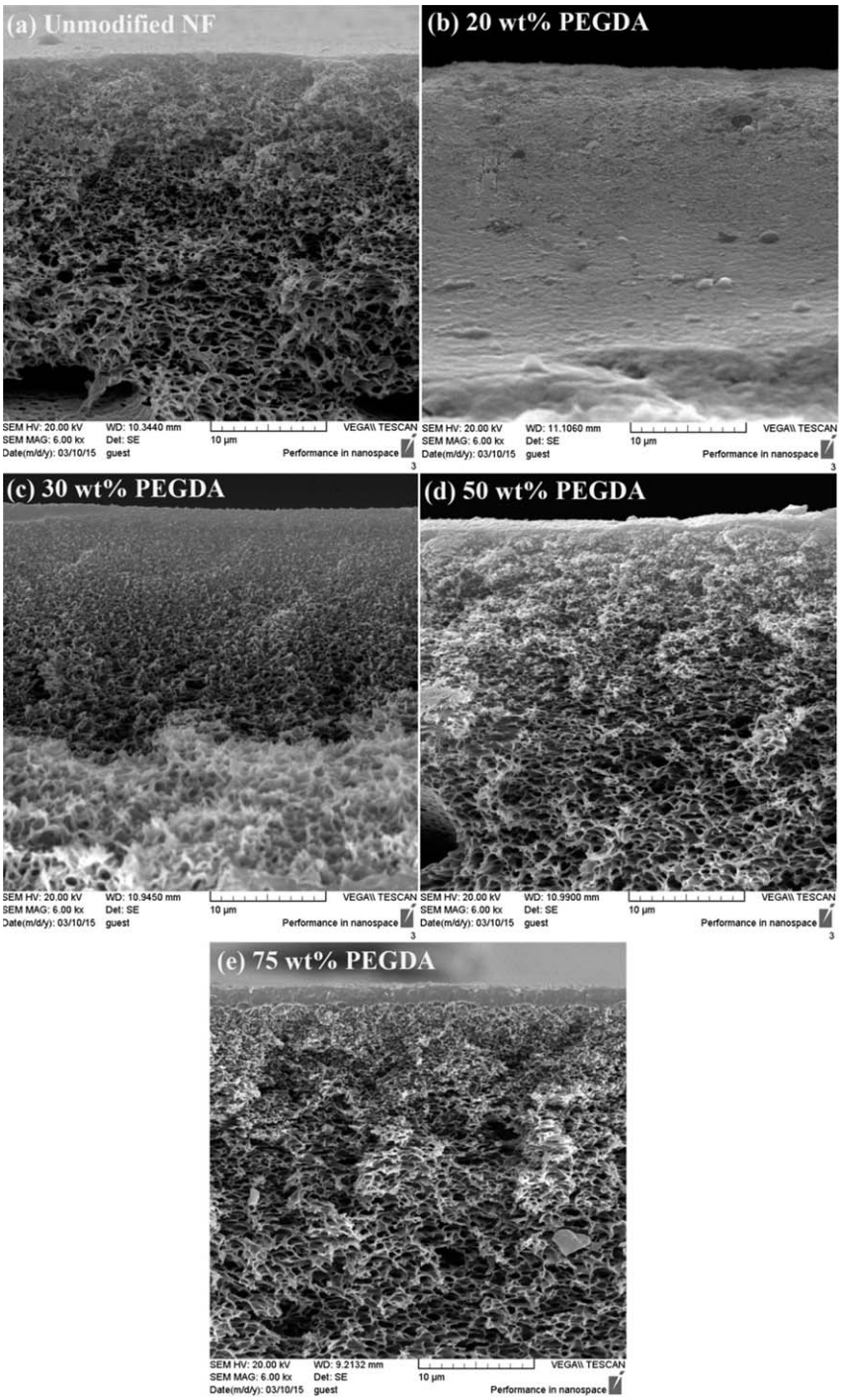

Figure 4. Cross-sectional SEM images of the membranes with different PEGDA concentrations: (a) bare NF, (b) 20 wt %, (c) 30 wt %, (d) 50 wt %, and (e) 75 wt %.

flux was permanently monitored during the testing period. The obtained flux profile was used to analyze the fouling behavior of the modified and unmodified PA NF membranes.

RESULTS AND DISCUSSION

PEGDA *In Situ* Polymerization on the NF Membrane Surface

The most effective parameter in the formation of a homogeneous PEGDA layer on the membrane surface is the monomer concentration. A series of commercial PA NF membranes was modified by UV photopolymerization at different monomer concentrations of PEGDA (20, 30, 50, and 75 wt %) during 5 min of UV-light exposure. The contact time between the PEGDA prepolymerization solution and the membrane surface was 10 min. The pure water flux values for the modified and unmodified membranes were measured by a crossflow setup at 10 bar of pressure. According to Figure 3, all of the PEGDA-

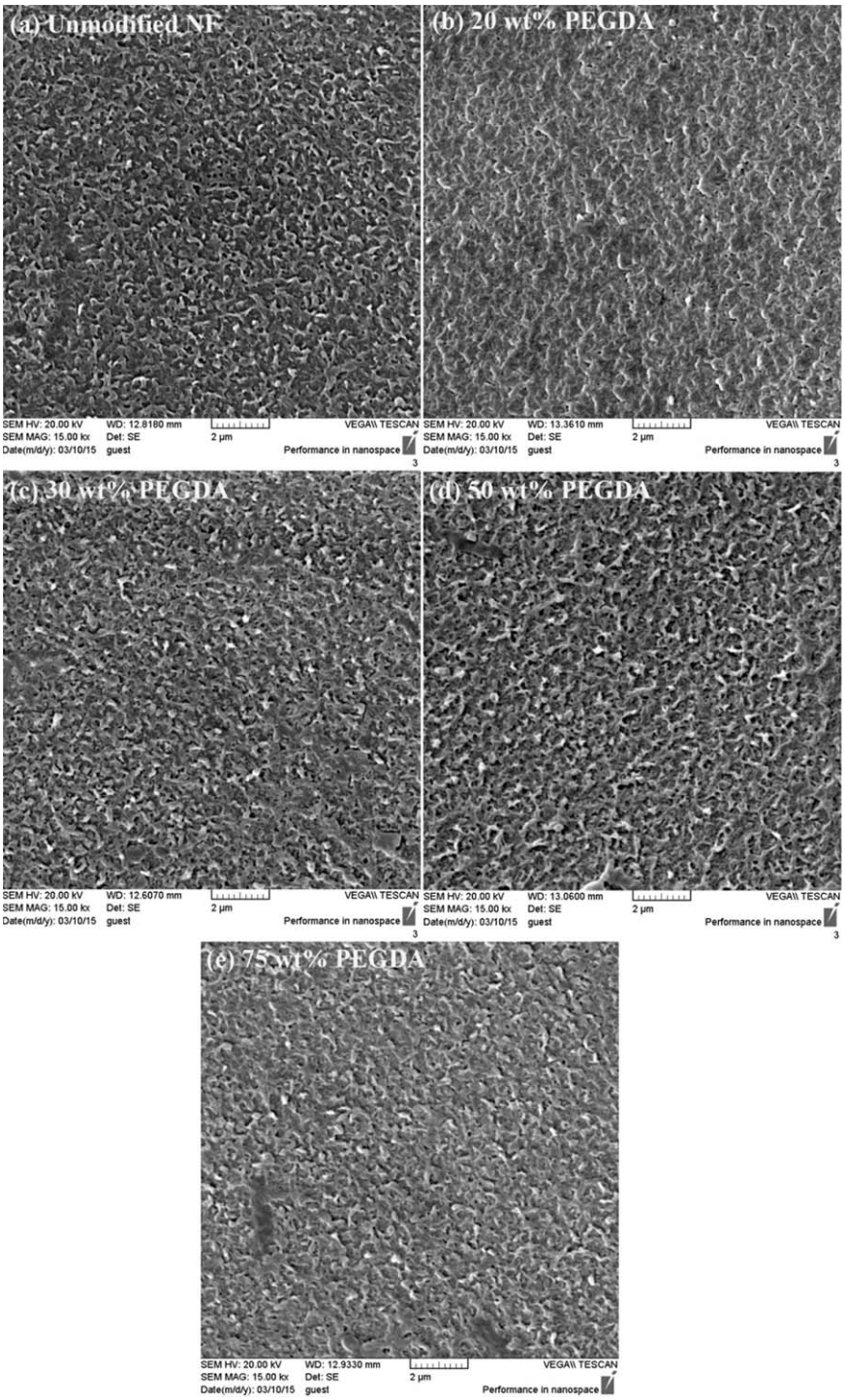

Figure 5. Surface SEM images of the PEGDA-modified membranes with different PEGDA concentrations: (a) bare NF, (b) 20 wt %, (c) 30 wt %, (d) 50 wt %, and (e) 75 wt %.

modified membranes under these conditions showed lower flux values than the bare NF membrane. This was due to an increase in the membrane intrinsic resistance with increasing thickness and probably pore blocking. Among the modified membranes, the 30 wt % PEGDA membrane presented the highest flux. This could have been related to the large pores of the modified membrane at low concentrations.[32] However, the 20 wt % PEGDA coated membrane had a lower flux than the 30 wt % PEGDA membrane. Cross-sectional SEM images of the PEGDA-modified membranes with different concentrations (presented in Figure 4) showed that in the 20 wt % PEGDA, the pores of the support were dense and seemed to be filled with dilute PEGDA solution. Probably, at a low concentration of PEGDA, the solution diffused to the membrane structure, and

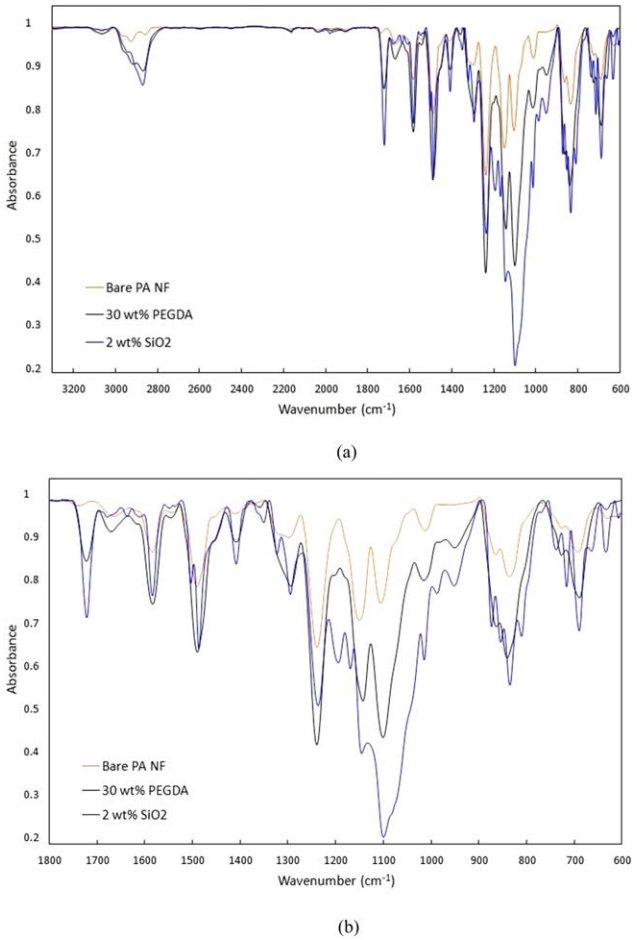

Figure 6. FTIR spectra of the unmodified and modified membranes in the presence and absence of SiO_2 nanoparticles. [Color figure can be viewed in the online issue, which is available at wileyonlinelibrary.com.]

polymerization happened in the interior layers of the modified membrane and caused more pore blocking than the 30 wt % membrane. However, in the 30 wt % membrane, the viscosity of the prepolymerization solution was higher, and it could not diffuse more.

Figure 4 also shows that with increasing PEGDA concentration, the thickness of the coated layer increased. In the 75 wt %

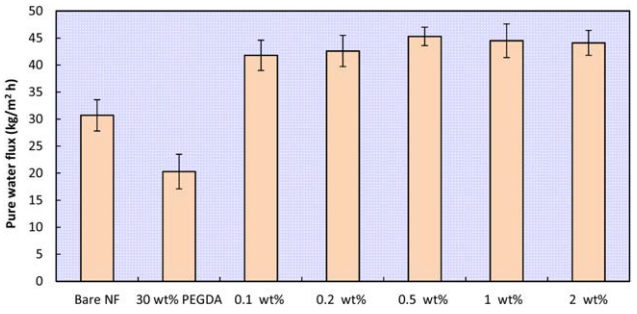

Figure 7. Effect of the SiO_2 concentration on the pure water flux of the 30 wt % PEGDA coated NF membrane. [Color figure can be viewed in the online issue, which is available at wileyonlinelibrary.com.]

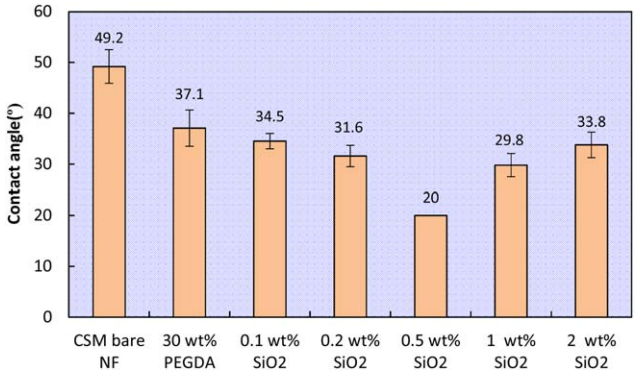

Figure 8. Static water contact angle of a 30 wt % PEGDA coated membrane in the presence of different SiO_2 nanoparticle concentrations. [Color figure can be viewed in the online issue, which is available at wileyonlinelibrary.com.]

PEGDA membrane, the thickness of the coated layer was about 3 μm. The increase in the PEGDA layer decreased the membrane flux. The flux of 75 wt % PEGDA was 5.2 kg/m^2 h; this was five times lower than that of the unmodified membrane. As shown in Figure 4(b), at the lowest concentration of the PEGDA (20 wt %), the thickness of the prepared coating layer was lower than 1 μm, which was not detectible with this resolution of SEM imaging.

The surface morphology of the modified membranes with different PEGDA concentrations was studied through SEM image analysis. As shown in Figure 5, the bare PA NF membrane had typical ridge-and-valley structures commonly observed in this type of PA membranes.[15] This nodular structure was similar to that observed for the PEGDA-modified membranes with few changes. For 20 wt % membranes, we observed that the surface became smoother, and the ridge-and-valley was filled with PEGDA hydrogels. However, for the 30 and 50 wt % PEGDA coated membranes, the surface again became rougher. We observed that some new regular nodules appeared on the modified membranes. This was probably due to the connection or aggregation of the PEGDA chains in the dry state.[18] After the *in situ* surface polymerization of the PEGDA chains, some regions were covered with new nodules. The same behavior was reported by Kang *et al.*[18] for the surface modification of a commercial PA RO membrane by carbodiimide-induced grafting with PEG derivatives. Similar morphological changes were also observed when PEG-like monomers were grafted onto RO membranes by plasma polymerization.[33]

The rougher surface of the 30 wt % membrane relative to the 20 wt % PEGDA membrane could have been another reason for its higher pure water flux. The rougher surface had a more active area for the penetration of water.

PEGDA concentrations of 10 and 100 wt % were also tested. In 10 wt %, the polymerization layer was not formed on the membrane or on a glass surface (the solution was cast on a glass surface and exposed to a UV lamp); this was due to the very low amount of PEGDA, which could not contact, together with polymerization. In 100 wt % PEGDA, the resulting membrane did not show permeation at 10 bar. The uniformity of a coated

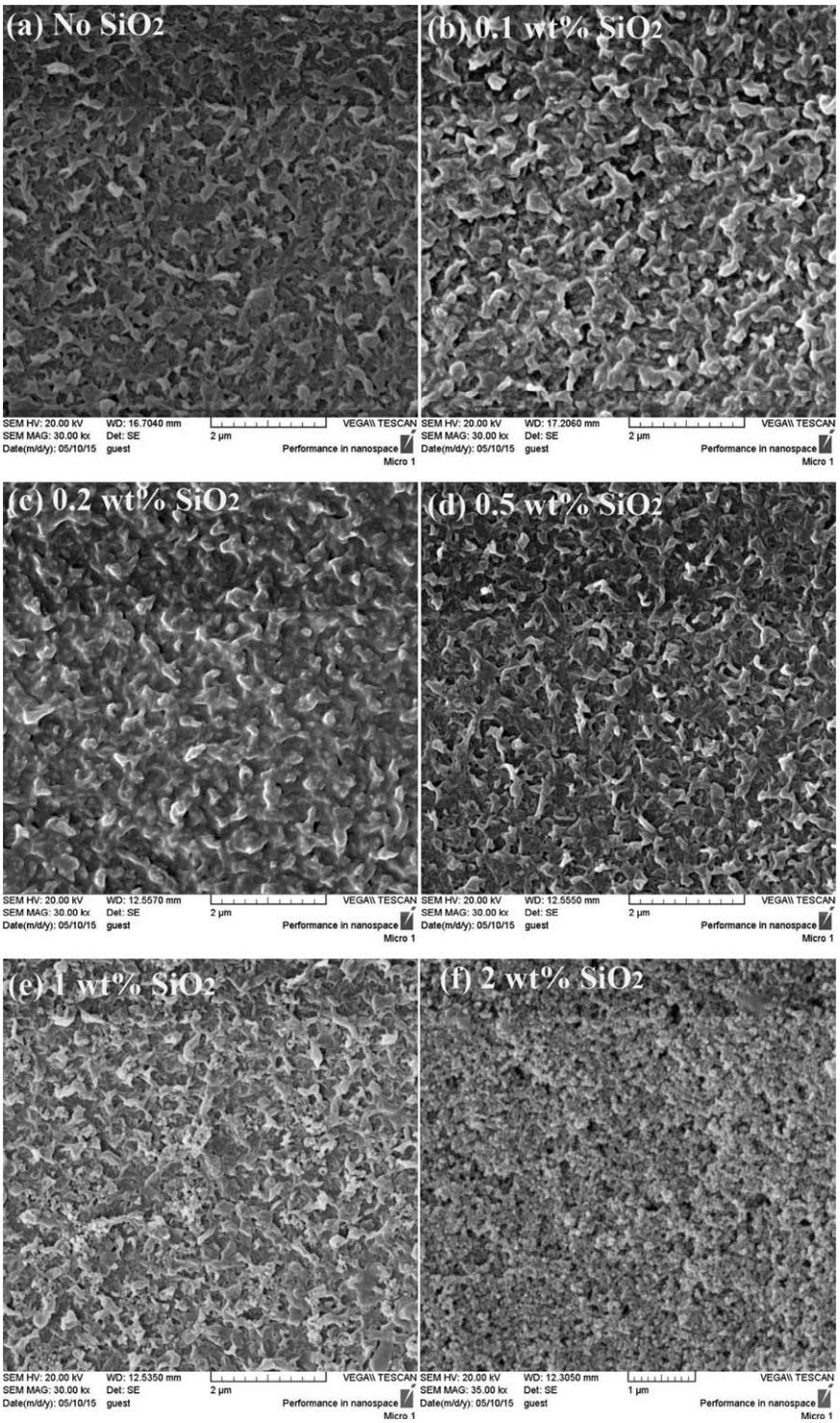

Figure 9. Surface SEM images of the modified membranes with 30 wt % PEGDA and different concentrations of SiO_2 nanoparticles: (a) no SiO_2, (b) 0.1 wt %, (c) 0.2 wt %, (d) 0.5 wt %, (e) 1 wt %, and (f) 2 wt %

polymer onto a modified membrane surface is usually vital to the control of the filtration effectiveness.

In conclusion, the grafted membrane with 30 wt % PEGDA had a lower pure water flux than the bare NF, and therefore, other parameters need to be optimized to increase the flux.

Effect of SiO_2 Nanoparticles in PEGDA

On the basis of the previous results, the membrane with 30 wt % PEGDA was selected as the optimum membrane, and SiO_2 nanoparticles were mixed into the PEGDA prepolymerization solutions and polymerized *in situ* on the bare NF membrane.

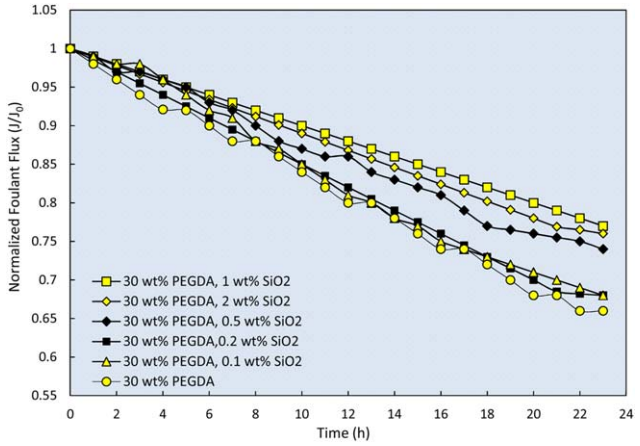

Figure 10. Effect of the amounts of SiO_2 nanoparticles on the normalized foulant permeate flux of the modified membrane with 30 wt % PEGDA (the averages of three replicates are presented). [Color figure can be viewed in the online issue, which is available at wileyonlinelibrary.com.]

FTIR measurement was conducted to determine the successful *in situ* polymerization of PEGDA and the incorporation of SiO_2 nanoparticles onto the membrane surface. Figure 6 illustrates the attenuated total reflection–FTIR spectra of the unmodified NF membrane, the modified membrane with 30 wt % PEGDA, and the 2 wt % SiO_2 containing PEGDA membrane.

The entire spectra showed almost the same attenuated total reflection–FTIR spectra as the polysulfone support layer with typical peaks at 1592 and 1110 cm^{-1} (aromatic double-bonded carbon), 1492 cm^{-1} (methyl groups), 1016 cm^{-1} (ester groups), and 694 and 1151 cm^{-1} (sulfone groups) and the PA selective layer with indicative peaks at 1660 cm^{-1} due to amide I (C═O stretch), 1545 cm^{-1} due to amide II (C—N stretch), and 1609 cm^{-1} due to PA aromatic ring breathing. Also, the peaks that appeared in the range 2800–3000 cm^{-1} were related to aromatic ═C—H stretching and aliphatic C—H stretching.[27,34]

In the presence of the PEGDA layer, the strong absorption band at 1105 cm^{-1} confirmed the stretched C—O structure, and the peak at 1724 cm^{-1} was related to the C═O stretched bond.

The FTIR spectrum for the 30 wt % PEGDA-modified membrane in the presence of SiO_2 nanoparticle showed absorption bands about 1103 cm^{-1} related to Si—O—Si stretched bond and 793 cm^{-1}, which resulted from symmetrical stretching vibrations of Si—O, whereas the membrane without SiO_2 nanoparticles did not have this peak.[35,36]

The results of the pure water flux of SiO_2 blended PEGDA membranes are depicted in Figure 7. With the addition of SiO_2 nanoparticles to the prepolymerization solution of 30 wt % PEGDA, the water flux of all of the prepared membranes was increased. The pure water flux was improved until the SiO_2 concentration was increased up to 0.5 wt %. Then, it partially decreased with increasing SiO_2 amount to 1 and 2 wt %. However, the water flux was still greater than that of the unfilled 30 wt % PEGDA.

The reason for increasing of the water flux by increasing SiO_2 nanoparticle concentration was attributed to the membrane hydrophilicity improvement, changes in the surface morphology, and an increase in the porosity of the PEGDA layer.

It is known that the membrane surface hydrophilicity is one of the most significant factors influencing membrane performance, and the contact angle test is a common test for determining the hydrophilic amount and the ability to wet the membrane surface. As indicated in Figure 8, the contact angle of the commercial PA membrane was 49.2°. The polymerization of the 30 wt % hydrophilic PEGDA layer reduced the contact angle to 37.1°. The increase in the SiO_2 nanoparticle led to a reduction in the contact angle and, therefore, an increase in the hydrophilic properties of the membrane.[37,38] The results show that 0.5 wt % SiO_2 had the highest pure water flux and a lower contact angle. The contact angle of the 0.5 wt % membrane was very low, and the angle between the water drop and membrane surface was not precisely measured. However, when the concentration of SiO_2 nanoparticles was greater than 0.5 wt %, the contact angle increased, and the pure water flux also decreased. This behavior was attributed to the agglomeration of the SiO_2 nanoparticles at higher concentrations, as shown in the surface SEM images depicted in Figure 9.

Figure 9 presents the surface SEM images of the modified membranes with 30 wt % PEGDA containing different amounts of SiO_2 nanoparticles (0.1, 0.2, 0.5, 1, and 2 wt % related to the PEGDA amount). As shown in the SEM micrographs, the microstructural surface morphologies of the membranes changed with the SiO_2 amount. The images illustrate that at lower concentration of SiO_2 nanoparticles, the membrane surface became relatively smooth, and at higher concentrations of SiO_2 nanoparticles (1 and 2 wt %), the aggregation of SiO_2 nanoparticles were obvious in the membrane surface. At higher SiO_2 loadings, the nanoparticles and the polymer-only phase interacted well with each other, and larger microstructures were shaped on the membrane surfaces.

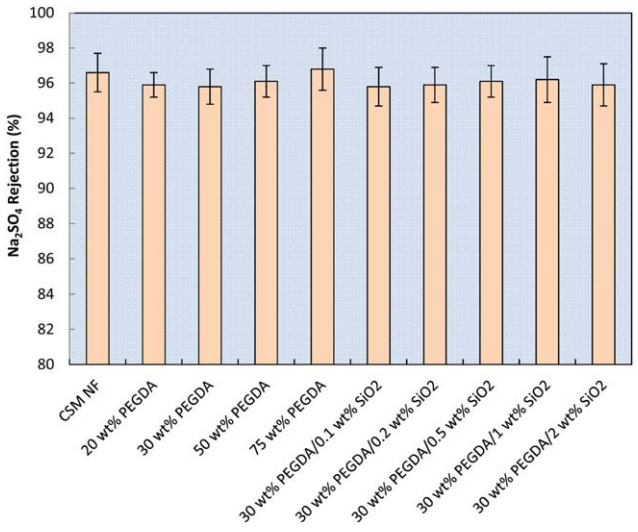

Figure 11. Na_2SO_4 rejection of the membranes (2000 ppm salt, 10 bar). [Color figure can be viewed in the online issue, which is available at wileyonlinelibrary.com.]

As shown in Figure 10, the normalized foulant flux plot was presented to show the fouling amount of the modified NF membranes by 30 wt % PEGDA prepolymerization solution in the presence of different concentrations of SiO_2 nanoparticles. The results were obtained for a 24-h fouling test with 500 mg/L BSA, 2000 mg/L Na_2SO_4, and 500 mg/L humic acid solution. The reduction of the foulant flux of the membranes containing SiO_2 nanoparticles was lower than that of the 30 wt % PEGDA pure membrane during the 24-h fouling test; this showed that the presence of SiO_2 nanoparticles decreased the fouling. When the SiO_2 nanoparticle concentration was increased, the fouling amount was decreased. The 1 wt % SiO_2 blended membrane had the highest amount of permeate flux of the foulant solution; however, the 2 wt % SiO_2 blended membrane presented the highest normalized foulant flux.

We concluded that the presence of SiO_2 nanoparticles reduced the foulant attachment to the membrane surface[39] and, therefore, improved the antifouling properties. Nevertheless, the higher concentration of the SiO_2 nanoparticles could block the membrane pore size and reduce the foulant flux.

Figure 11 presents the Na_2SO_4 rejection results of the bare NF and modified membranes by the PEGDA layer. As shown, the obtained rejection showed that the coating layer was not induced any defect in the NF PA layer. The NF membrane rejection was controlled by the pore size and surface charge.[40] The coating of the PEGDA layer probably reduced the pore size and increased the selective layer thickness. However, this change was not significant, and it did not induce membrane rejection.

CONCLUSIONS

In this study, a commercial PA NF membrane was modified by the *in situ* polymerization of a hydrophilic monomer of PEGDA blended with SiO_2 nanoparticles. The effect of the PEGDA coating on the performance of the modified membrane was related to its concentration. With increasing PEGDA concentration, the amount of pure water flux decreased because of the formation of a thicker layer. The flux amounts of the modified membranes by PEGDA were improved in the presence of SiO_2 nanoparticles. Also, the fouling decreased with increasing SiO_2 nanoparticle concentration. We concluded that the coating of both PEGDA and SiO_2 on the PA TFC membranes improved the performance of the resulting membranes.

ACKNOWLEDGMENTS

The authors thank Kharazmi University for all the support that it provided. They also sincerely appreciate Petrochemical Research and Technology Co. (Tehran, Iran) for its financial support of this project (contract grant number 0870289215).

REFERENCES

1. Nanda, D.; Tung, K.-L.; Li, Y.-L.; Lin, N.-J.; Chuang, C.-J. *J. Membr. Sci.* **2010**, *349*, 411.
2. Jin, L.; Shi, W.; Yu, S.; Yi, X.; Sun, N.; Ma, C.; Liu, Y. *Desalination* **2012**, *298*, 34.
3. Asatekin, A.; Olivetti, E. A.; Mayes, A. M. *J. Membr. Sci.* **2009**, *332*, 6.
4. Zazouli, M. A.; Nasseri, S.; Ulbricht, M. *Desalination* **2010**, *250*, 688.
5. Lapointe, J. F.; Gauthier, S. F.; Pouliot, Y.; Bouchard, C. *J. Membr. Sci.* **2005**, *253*, 89.
6. Tang, C. Y.; Kwon, Y. N.; Leckie, J. O. *J. Membr. Sci.* **2007**, *290*, 86.
7. Nghiem, L. D.; Hawkes, S. *Sep. Purif. Technol.* **2007**, *57*, 176.
8. Madaeni, S. S.; Zinadini, S.; Vatanpour, V. *Sep. Purif. Technol.* **2011**, *80*, 155.
9. Sagle, A. C.; Van Wagner, E. M.; Ju, H.; McCloskey, B. D.; Freeman, B. D.; Sharma, M. M. *J. Membr. Sci.* **2009**, *340*, 92.
10. Zhang, Y.; Su, Y.; Chen, W.; Peng, J.; Dong, Y.; Jiang, Z.; Liu, H. *J. Membr. Sci.* **2011**, *382*, 300.
11. Hyun, J.; Jang, H.; Kim, K.; Na, K.; Tak, T. *J. Membr. Sci.* **2006**, *282*, 52.
12. Asatekin, A.; Kang, S.; Elimelech, M.; Mays, A. *M. J. Membr. Sci.* **2007**, *298*, 136.
13. Kim, E.-S.; Yu, Q.; Deng, B. *Appl. Surf. Sci.* **2011**, *257*, 9863.
14. Kim, I.-C.; Jeong, B.-R.; Kim, S.-J.; Lee, K.-H. *Desalination* **2013**, *308*, 111.
15. Safarpour, M.; Khataee, A.; Vatanpour, V. *J. Membr. Sci.* **2015**, *489*, 43.
16. Miao, J.; Zhang, L.-C.; Lin, H. *Chem. Eng. Sci.* **2013**, *87*, 152.
17. Harris, J. M. Poly(ethylene glycol) Chemistry: Biotechnical and Biomedical Applications; Plenum: New York, **1992**.
18. Kang, G.; Yu, H.; Liu, Z.; Cao, Y. *Desalination* **2011**, *275*, 252.
19. Thom, V.; Jankvoa, K.; Ulbricht, M.; Kops, J.; Jonsson, G. *Macromol. Chem. Phys.* **1998**, *199*, 2723.
20. Zou, X. P.; Kang, E. T.; Neoh, K. G. *Surf. Coat. Technol.* **2002**, *149*, 119.
21. Nie, F. Q.; Xu, Z. K.; Huang, X. *J. Langmuir* **2003**, *19*, 9889.
22. Lin, H. Q.; Wagner, E. V.; Freeman, B. D.; Toy, L. G.; Gupta, R. P. *Science* **2006**, *311*, 639.
23. Lin, H. Q.; Kai, T.; Freeman, B. D.; Kalakkunnath, S.; Kalika, D. S. *Macromolecules* **2005**, *38*, 8381.
24. Lin, H. Q.; Freeman, B. D. *Macromolecules* **2005**, *38*, 8394.
25. Lin, H. Q.; Wagner, E. V.; Swinnea, J. S.; Freeman, B. D.; Pas, S. J.; Hill, A. J.; Kalakkunnath, S.; Kalika, D. S. *J. Membr. Sci.* **2006**, *276*, 145.
26. Ju, H.; McCloskey, B. D.; Sagle, A. C.; Wu, Y. H.; Kusuma, V. A.; Freeman, B. D. *J. Membr. Sci.* **2008**, *307*, 260.
27. Kang, G.; Cao, Y.; Zhao, H.; Yuan, Q. *J. Membr. Sci.* **2008**, *318*, 227.
28. Madaeni, S. S.; Zinadini, S.; Vatanpour, V. *J. Membr. Sci.* **2011**, *380*, 155.
29. Garcia-Ivars, J.; Iborra-Clar, M.-I.; Alcaina-Miranda, M.-I.; Mendoza-Roca, J.-A.; Pastor-Alcañiz, L. *Sep. Purif. Technol.* **2014**, *135*, 88.

30. Zhang, S.; Qiu, G.; Ting, Y. P.; Chung, T.-S. *Colloids Surf. A* **2013**, *436*, 207.
31. Vatanpour, V.; Shockravi, A.; Zarrabi, H.; Nikjavan, Z.; Javadi, A. *J. Ind. Eng. Chem.* **2015**, *30*, 342.
32. Wu, Y. H.; Park, H. B.; Kai, T.; Freeman, B. D.; Kalika, D. S. *J. Membr. Sci.* **2010**, *347*, 197.
33. Zou, L.; Vidalis, I.; Steele, D.; Michelmore, A.; Low, S. P.; Verberk, J. Q. J. C. *J. Membr. Sci.* **2011**, *369*, 420.
34. Kalakkunnath, S.; Kalika, D. S.; Lin, H. Q.; Freeman, B. D. J. *Polym. Sci. Part B: Polym. Phys.* **2006**, *44*, 2058.
35. Wu, C. M.; Xu, T. W.; Yang, W. H. *J. Membr. Sci.* **2003**, *224*, 117.
36. Xing, L.; Guo, N.; Zhang, Y.; Zhang, H.; Liu, J. *Sep. Purif. Technol.* **2015**, *146*, 50.
37. Guan, K. *Surf. Coat. Technol.* **2005**, *191*, 155.
38. Wei, X.; Wang, Z.; Chen, J.; Wang, J.; Wang, S. *J. Membr. Sci.* **2010**, *346*, 152.
39. Jadav, G. L.; Singh, P. S. *J. Membr. Sci.* **2009**, *328*, 257.
40. Mehdipour, S.; Vatanpour, V.; Karimini, H.-R. *Desalination* **2015**, *362*, 84.